5-20-1994

The Cataclysmic Variable HX Pegasi = PG 2337 + 123: Caught on the Rise to Maximum

F. A. Ringwald
Dartmouth College

Mon. Not. R. Astron. Soc. **270,** 804–810 (1994)

The cataclysmic variable HX Pegasi = PG 2337 + 123: caught on the rise to maximum

F. A. Ringwald[1,2]★

[1] *Department of Physics, Keele University, Keele, Staffordshire ST5 5BG*
[2] *Department of Physics and Astronomy, Dartmouth College, Hanover, New Hampshire 03755-3528, USA*

Accepted 1994 May 12. Received 1994 May 5; in original form 1993 May 20

ABSTRACT

A radial velocity study of the Hα emission line of the cataclysmic variable HX Peg = PG 2337 + 123 shows that its orbital period is 0.2008 ± 0.0005 d (4.82 h). Magnitudes from Harvard College Observatory archive plates suggest that it is either a dwarf nova or a VY Scl star. The quiescent spectrum shows K I $\lambda\lambda$7665, 7699 Å in absorption, consistent with the presence of an unusual subdwarf-K mass-losing star.

At the beginning of the second night of the run, O I λ7773 Å was in absorption. Near midnight, the continuum rose rapidly into maximum, with time-resolved red spectra taken throughout. This is the second-ever example of time-resolved spectroscopy of a cataclysmic variable's rise from minimum to a high state (after that of Mansperger & Kaitchuck), and the first with red spectra.

Key words: accretion, accretion discs – binaries: spectroscopic – stars: individual: HX Peg = PG 2337 + 123 – novae, cataclysmic variables.

You sure must live right having HX Peg sit up and perform for you like that.
W. Liller (private communication)

1 INTRODUCTION

Dwarf novae are a class of cataclysmic variables (CVs) that show outbursts that peak 2–5 mag above quiescent brightness. These last for days to weeks and recur over weeks to months. Observation of these outbursts is complicated by their being only quasi-periodic: there are large dispersions in their recurrence times, outburst durations and amplitudes (Warner 1987). Dwarf nova outbursts are thought to be accretion-powered, in contrast to the nuclear-powered eruptions of classical novae, although the mechanism for dwarf nova outbursts has long been controversial. The competing models are thermal instabilities in the accretion disc, which feeds the white dwarf (Osaki 1974), or modulated mass transfer from its K–M dwarf companion, which feeds the disc (Bath 1973). The subclasses of dwarf novae are named after the prototypes U Gem, Z Cam and SU UMa, and to distinguish them requires detailed long-term light curves. Another class of CVs, the VY Scl stars, are also called antidwarf novae, since they are usually bright but fade unpredictably. For reviews on theory and phenomenology, see Smak (1984), Mattei (1990) and la Dous (1993).

This paper reports a radial velocity study of HX Pegasi = PG 2337 + 123 = 'A Blue Variable at High Latitude' (Green, Greenstein & Boksenberg 1976, hereafter GGB76), carried out while investigating CVs found by the Palomar-Green survey (Green, Schmidt & Liebert 1986; Ringwald 1993). On the first night, HX Peg was near $R = 15$, estimated by its appearance on the TV monitor, and had strong emission lines. Halfway through the second night, its continuum rose rapidly, overwhelming the lines. On the third night, HX Peg was near $R = 12$–13, with weak emission lines.

This is the second-ever example of such time-resolved spectroscopy of a cataclysmic variable, caught on the rise from minimum to a high state, after that of Mansperger & Kaitchuck (1990, hereafter MK90) of the rise to outburst of the dwarf nova TW Vir. It is the first with red spectra, documenting the behaviour of O I λ7773 Å. One might hope to use these spectra to find where the brightening occurs in the disc, and how it propagates.

This object's photometric behaviour is discussed in Section 2, and magnitudes measured by L. E. Chaisson from Harvard College Observatory archive plates are presented. The spectroscopic observations are described in Section 3, with a journal given in Table 1. The radial velocity study is

★ Internet: far@astro.keele.ac.uk

presented in Section 4, with results summarized in Table 2. The quiescent spectrum and evidence for an unusual subdwarf-K mass-losing star are reported in Section 5. The rise from quiescence to maximum is described in Section 6, with overall discussion in Section 7.

2 PHOTOMETRIC BEHAVIOUR

The discovery and photometric properties of HX Peg are described by GGB76, who include a finding chart and note spectral variability on a time-scale of minutes. Greenstein, Arp & Shectman (1977, hereafter GAS77) show spectra varying on a time-scale of months. When the star is faint, the Balmer and He I lines show up in strong, broad emission. When the star is bright, these lines weaken considerably, perhaps even going into absorption. This variability is consistent with HX Peg being either a dwarf nova or a VY Scl star. So is irregular photometric variability over days to years, between $m_{pg} = 13.2$ and 16.5, noted in a study with the Harvard College Observatory plate archive (Liller & Eachus 1976).

Fig. 1 presents this archival light curve for the first time, it having been described only briefly by Liller & Eachus (1976). The light curve covers 1895–1953 and 1970–1975.

Table 1. Hα velocity, equivalent width and continuum slope.

MHJD[a]	V[b] (km s^{-1})	W (Å)	α[c]	MHJD[a]	V[b] (km s^{-1})	W (Å)	α[c]	MHJD[a]	V[b] (km s^{-1})	W (Å)	α[c]
8547.603	54	25.4	2.7	8547.840	−30	21.0	3.0	8548.752	48	3.5	2.2
8547.614	18	20.4	2.4	8547.851	−105	26.1	1.3	8548.764	94	2.4	3.4
8547.625	7	23.3	2.2	8547.862	−142	23.8	2.0	8548.775	−9	4.2	3.0
8547.637	−57	23.3	1.1	8547.873	−66	25.3	1.6	8548.787	124	3.0	2.6
8547.648	−51	17.6	−1.7	8547.884	−114	22.1	1.4	8548.798	330	1.6	3.0
8547.660	−42	20.0	−1.2	8547.895	−119	23.7	2.1	8548.810	126	1.6	3.4
8547.670	−66	21.2	−1.4	8548.581	158	14.3	1.7	8548.821	92	1.7	3.3
8547.682	−84	22.8	1.0	8548.592	75	13.7	1.8	8548.833	−186	1.6	3.5
8547.693	−102	19.7	−0.3	8548.604	125	15.7	1.9	8548.844	72	1.5	3.5
8547.704	−2	25.7	0.8	8548.615	77	14.0	2.2	8548.856	195	0.7	3.4
8547.715	68	21.8	−0.5	8548.627	26	9.9	2.2	8548.867	−80	1.2	3.7
8547.727	48	25.0	0.9	8548.638	−33	10.2	1.2	8548.879	−236	0.8	4.2
8547.738	140	28.1	−0.2	8548.649	−88	9.7	2.4	8548.890	319	0.5	4.2
8547.750	170	29.4	1.6	8548.660	−63	9.5	2.3	8549.609	242	1.9	3.0
8547.760	128	22.9	0.1	8548.672	−137	10.2	2.2	8549.622	143	2.3	3.1
8547.772	102	21.3	2.1	8548.683	−116	9.0	2.8	8549.634	166	1.9	2.6
8547.783	134	19.9	2.2	8548.695	−20	8.0	2.3	8549.644	110	2.6	3.0
8547.795	124	17.7	1.3	8548.706	16	4.9	2.5	8549.656	31	1.9	3.4
8547.806	111	21.4	1.3	8548.718	−15	6.0	2.4	8549.667	−57	3.0	3.1
8547.817	3	22.7	0.8	8548.729	45	6.7	2.3				
8547.828	−11	27.5	2.0	8548.741	−17	6.7	3.7				

[a]Heliocentric Julian Date of mid-integration, minus 244 0000.
[b]Measured with Shafter (1983) algorithm, Gaussian separation 1370 km s^{-1}.
[c]Index of power-law $F_\lambda = k\lambda^{-\alpha}$ fit to continuum over $\lambda\lambda$6350–6450 and 6750–6850 Å.

Table 2. HX Peg – derived orbital parameters[a].

Object	P_{orb} (days)	K_{em} (km s^{-1})	γ_{em} (km s^{-1})	T_0 (HJD − 2440000)	σ (km s^{-1})
Hα[b]					
October 18 only[c]	(0.2008)	125 ± 10	27 ± 7	8548.721 ± 0.004	34
Before rapid rise[d]	0.2008 ± 0.0005	125 ± 8	29 ± 6	8548.721 ± 0.002	34
After rapid rise[e]	(0.2008)	81 ± 10	58 ± 30	8548.746 ± 0.016	138
After, points deleted[f]	(0.2008)	109 ± 20	43 ± 11	8548.747 ± 0.004	42
K I λ 7665[g]		K_{abs}	γ_{abs}		
(coadded)	(0.2008)	214 ± 78	−188 ± 55	8548.64 ± 0.01	141

[a]Velocities fitted to $V(t) = \gamma + K \sin[2\pi(t - T_0)/P_{orb}]$; all errors are to 68 per cent confidence (see Thorstensen & Freed 1985).
[b]Measured with Shafter (1983) algorithm, Gaussian separation 1370 km s^{-1}.
[c]MHJD 8547.895 and all previous spectra (1991 October 18 = MHJD 8547).
[d]First 39 velocities, to rapid rise (MHJD 8548.706 and all previous spectra).
[e]Velocities 40–61 (MHJD 8548.718 and all subsequent spectra).
[f]The velocities removed were at MHJD − 8540 = 8.775, 8.798, 8.833, 8.856, 8.879, 8.890 and 9.609.
[g]Fit to absorption line, Schneider & Young (1980) algorithm, Gaussian width 640 km s^{-1}.

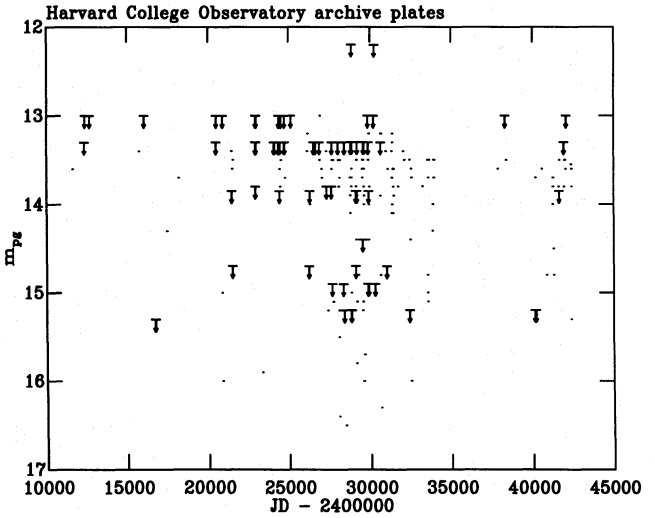

Figure 1. Photographic magnitudes and upper limits from Harvard College Observatory archive plates, compiled by L. E. Chaisson.

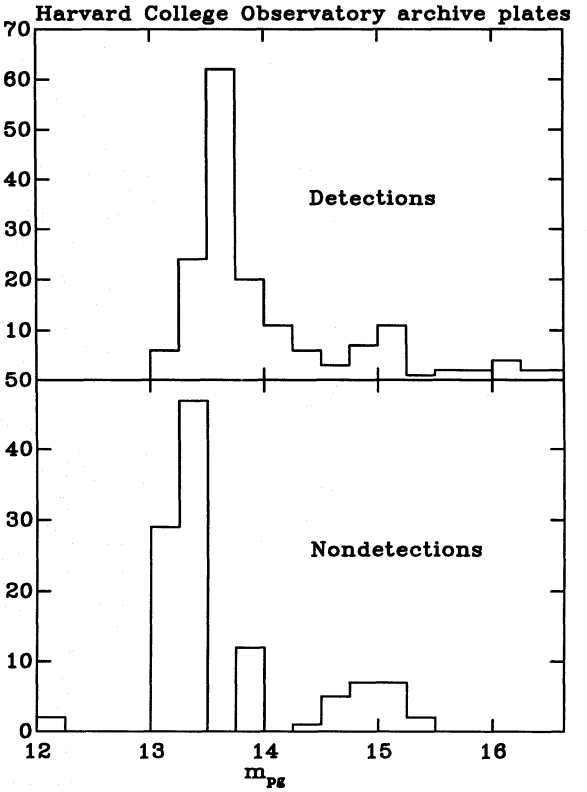

Figure 2. Histogram of magnitudes from Fig. 1, of both detections and non-detections. While 92 per cent of the detections and 60 per cent of the non-detections had $m_{pg} < 13.75$, the star can clearly have $m_{pg} > 15.5$.

Plates both from sky patrols (BM, RB, RH, DNB and DSB) and from series programmes (MA, MC, I and IR) were examined, with a total of 163 detections. There were also 112 non-detections, in which HX Peg was fainter than various plate limits spread over $12.2 < m_{pg} \lesssim 16.5$. Times between observations also varied widely, but they were generally separated by weeks or longer.

Fig. 2 shows that, while $m_{pg} < 13.75$ in 92 per cent of the detections and in 60 per cent of the non-detections, HX Peg reached $m_{pg} > 15.5$ in all plates with limiting magnitudes that faint. Eclipses can cause dipping behaviour, and there never has been a systematic search for them in HX Peg. It is unlikely, though, that eclipses are the sole cause of this star's variability, since the time-scale for the observed rise to maximum is longer than the orbital period of 4.82 h, found in Section 4. Also, the long-term CCD light curve of Honeycutt et al. (1994), taken once or twice nightly over three sets of several weeks spanning 1.6 yr overall, shows smooth day-to-day variations in brightness, not the apparently random variability expected of eclipses.

The orbital period is more likely to belong to a dwarf nova, since all orbital periods known securely for VY Scl stars are between 3.2 and 3.9 h (Ritter 1990). This is exactly the period regime where dwarf novae are rare, for unknown reasons (Shafter, Wheeler & Cannizzo 1986). However, only further and more thorough long-term monitoring can distinguish the exact outburst type.

3 SPECTROSCOPIC OBSERVATIONS

HX Peg was observed with the 1.3-m McGraw-Hill telescope and the Mark IIIa (black) spectrograph at Michigan–Dartmouth–MIT Observatory, Kitt Peak, Arizona, on 1991 October 18–20 UT. Observational procedure was similar to that of Thorstensen & Freed (1985), and data reductions were carried out as by Thorstensen et al. (1991b), with exceptions noted.

Only the first night was clear, perhaps even photometric, although volcanic dust from Mt Pinatubo was lighting up the sunset. Instrument rotation on the McGraw-Hill telescope was not used, so spectrophotometry may have suffered from differential refraction through the 2.2-arcsec slit. Nevertheless, this setup has worked well for radial velocity studies of other CVs (Thorstensen et al. 1991b; Thorstensen, Davis & Ringwald 1991a; Beuermann et al. 1992), and the long slit did provide for accurate digital sky subtraction. The detector was a TI-4849 CCD, mounted inside the BRICC camera (Luppino 1989). A 300 line mm^{-1} grism, blazed at $\lambda 6400$ Å, was used. A Hoya Y-50 order-blocking filter suppressed overlap with the red setup, which covered $\lambda\lambda 6200$–9000 Å. At 5 Å $pixel^{-1}$ along the dispersion, this gave 11-Å resolution FWHM. The wavelength scale was calibrated to within 0.1 Å, and reproducible to 0.05 Å, with fifth-order polynomial fits to the wavelengths of the lines of Ne, Ar and Xe lamps, taken at the beginning of each night. Wavelength stability was assured with Ne lamps, taken nominally every 30 min while observing, between target exposures. Object exposures were 15 min long. Flux standards (Oke 1974) were taken to remove the instrumental signature from the spectra. Hot stars (Oke & Gunn 1983) were also observed to map and remove telluric absorption features (see Wade & Horne 1988). Sometimes these bands did not divide out perfectly, causing wrinkles in the spectra near $\lambda 7600$ Å.

4 RADIAL VELOCITY STUDY

The radial velocities were measured with the method of Shafter (1983), in which a positive and a negative Gaussian

of specified width and separation were convolved with the Hα emission line, with the centroid of this convolution taken to be the radial velocity. This method had the advantage of being able to ignore erratic low-velocity variations, perhaps coming from poorly understood gas motions in the accretion disc. Instead, attention was focused on the overall motion of the system, to find the orbital period. The velocity measurements used a Gaussian width of 2.8 pixel, or 640 km s^{-1}, and a Gaussian separation of 1370 km s^{-1}, to maximize K_{em}/σ (see Table 2). Errors for the individual velocities were ± 10–15 km s^{-1}, estimated both by Monte Carlo simulations and by these being the smallest velocities reproducible with this technique.

Throughout the first night, Hα was in strong emission, with $I_{peak}/I_{cont} \approx 1.8$, as in the minimum spectrum of GAS77. Strong lines made the measurement of radial velocities easier, so spectra were taken throughout the night, in order to build up a long time baseline for an orbital period determination. On the second night, the time-resolved observations were continued, to obtain enough velocities to resolve the phase unambiguously and avoid cycle-count aliasing. The lines were still strong enough to allow velocity measurements with no problem, even though the continuum had brightened during the intervening day, Hα having $I_{peak}/I_{cont} \approx 1.6$ at the beginning of this night.

A Lomb–Scargle periodogram (Press et al. 1992) was computed of the first 39 Hα velocities, up to MHJD = HJD − 244 0000 = 8548.706. About 2 h after this, the brightening continuum made velocities difficult to measure, so subsequent velocities were not used for orbital period determination. The periodogram (Fig. 3) clearly showed a preferred period of 0.2008 d (4.82 h), with this peak standing out over its 1 cycle d^{-1} aliases. A least-squares fit to a sinusoid (Fig. 4) gave the parameters listed in Table 2, with errors for the ensemble estimated internally with the likelihood-ratio test of Cash (1979).

With the orbital period measured with the emission lines, the first 39 spectra were binned into eight phase bins to build the signal-to-noise ratio (S/N) up to an average of 55 near Hα in each binned spectrum. This made possible a radial velocity study with the K I λ7665-Å absorption line, with resulting parameters shown in Table 2. The line was measured with the method of Schneider & Young (1980), in which the line was convolved with the derivative of a Gaussian and the centroid of this convolution taken as the radial velocity. With a narrow Gaussian, of 640 km s^{-1} FWHM, this sensed the bottom of the V-shaped profile of this absorption line.

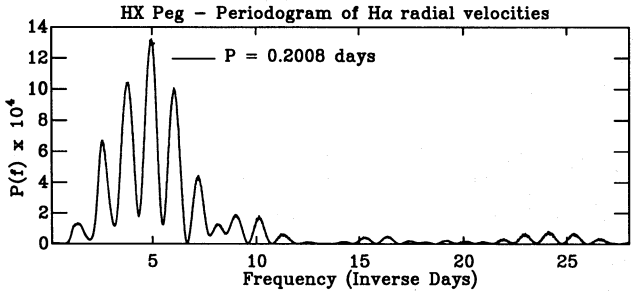

Figure 3. Periodogram of the first 39 Hα radial velocities, ending at MHJD 8548.706, measured by double-Gaussian algorithm (Shafter 1983) with a separation of 1370 km s^{-1}. The periodicity at 0.2008 d (4.82 h) is obvious, with the peak corresponding to it at 4.98 cycle d^{-1} towering over the 1 cycle d^{-1} aliases.

5 MINIMUM SPECTRUM

The bottom trace of Fig. 5 depicts the average spectrum during the first night, for which S/N = 110. For the individual spectra, S/N = 25 near Hα, and S/N = 21 near K I $\lambda\lambda$7665, 7699 Å. This minimum spectrum resembled that of a quiescent dwarf nova, with strong, broad Hα in emission. The He I $\lambda\lambda$6678, 7065-Å lines were also in broad emission, with double peaks of separation 750 and 900 km s^{-1}, respectively. Average equivalent widths for Hα and He I $\lambda\lambda$6678, 7065 Å were 26 ± 1, 2 ± 1, and 2 ± 1 Å, respectively; FWHM linewidths were 1240 ± 50, 2000 ± 90 and 1700 ± 80 km s^{-1}. The O I λ7773-Å feature was not obvious.

Features from this CV's mass-losing star included the K I $\lambda\lambda$7665, 7699-Å lines. These lines were deeper than any TiO band that might have been present at λ7600 Å, suggesting a spectral type earlier than M1. All the flux-deficit ratios of Wade & Horne (1988) indicated a spectral type earlier than M0.5, with $d_\nu(\lambda 7165)/c_\nu(\lambda 7500) = d_\nu(\lambda 7165)/c_\nu(\lambda 7165) = 0.063$ and $d_\nu(\lambda 7665)/c_\nu(\lambda 7500) = d_\nu(\lambda 7665)/c_\nu(\lambda 7665) = 0.0052$.

The CH absorption feature at $\lambda\lambda$4290–4314 Å, a spectral type indicator for G stars, was detected by GGB76 when HX Peg was near minimum. With the orbital period found in Section 5, an M2 dwarf should fit inside the Roche lobe of this star (Patterson 1984). If one finds a CV red star with an anomalous spectral type, one should expect to find an anomalously later type, from a red star that is evolved or at least out of thermal equilibrium from mass loss – not an earlier type. This supports the conclusion of GAS77 that the red star in HX Peg is a subdwarf-K star, based on a spectrophotometric trace they took during a deep minimum. They found $M_V = 7.5 \pm 0.2$ in quiescence, which at $m_V = 16.6$ means this star is in the Galactic halo, at a distance of 660 ± 60 pc. While a search for halo CVs has been undertaken by Howell & Szkody (1990), none so far has shown a mass-losing component that is a cool subdwarf.

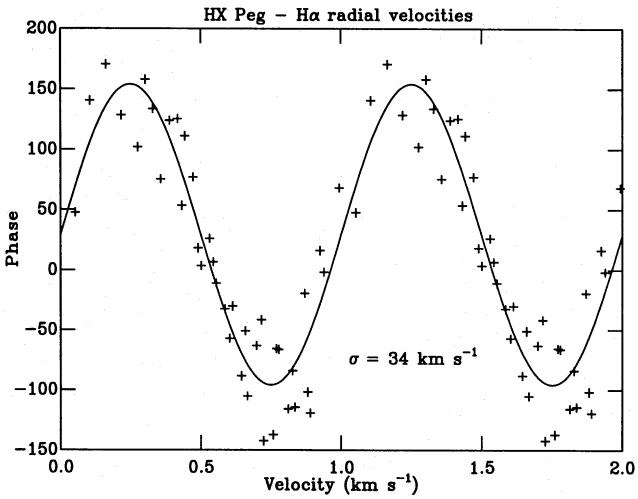

Figure 4. The first 39 Hα radial velocities, plotted about the orbital phase. All points are plotted twice for clarity.

6 FROM MINIMUM TO HIGH STATE

Throughout the second night, Hα changed in profile and equivalent width due to the brightening continuum (see Figs 5 and 6). Halfway through this night, at MHJD = 8548.787, this continuum brightening was especially rapid. He I disappeared completely, although the emission core of the Hα line was always at least weakly present.

The radial velocity curves from the entire first night and from the first 39 velocities were not significantly different (see Table 2). Seven velocities fell substantially off this sinusoid, by over 100 km s^{-1}. These were the velocities taken at MHJD − 8540 = 8.775, 8.798, 8.833, 8.856, 8.879, 8.890 and 9.609. All seven of these velocities occurred during or after the rapid rise to the high state, and were attributable to either line profile changes or the brightened continuum interfering with radial velocity measurements. With these seven velocities removed, the radial velocity curve's fit to a sinusoid improved considerably (see Table 2).

Equivalent widths for the Hα emission line were measured, with errors of ±0.5 Å (see Table 1). From quiescence to maximum, their fractional variation decreased by a factor of 3, and the standard deviation of their fit to a line decreased by a factor of 2 (Fig. 6). This was similar to the behaviour of the approximate *B* light curve of TW Vir observed by MK90 (see their fig. 1), perhaps resulting from increased mass-flow through the disc during outburst masking the bright spot, where the gas stream hits the disc. Even so, the equivalent widths in quiescence did not fit well to any sinusoid with the orbital period (to less than 38 per cent confidence), and the ratio of the equivalent widths' semi-amplitude to the standard deviation of the fit was only 0.43.

The Hα equivalent width curve shows a kink just at the rapid rise at MHJD = 8548.787. A sudden transition invites fitting of two lines: if a line is fitted to all 28 equivalent widths of this second night, the standard deviation of the fit is 1.4 Å. If two different lines are fitted (see Fig. 6) to the first 19 and to the last nine equivalent widths, the standard deviations of these fits are 1.3 and 0.3 Å, respectively.

At MHJD = 8548.695, about 2 h before the kink, a blue emission wing became noticeable on Hα. This wing protruded to about 1500 km s^{-1} from the line centre, and shows up in the average spectrum of the rapid rise (see Fig. 5). Beginning with the rapid rise, absorption wings developed about Hα, with cores ±750 km s^{-1} from the line centre. These remained for the rest of the night and for the next night, and are noticeable in Fig. 5. In contrast to the findings of MK90, the Hα emission line did not become appreciably narrower until immediately after the rapid rise, when it went from 1100 to 800 km s^{-1} FWHM. Hα never went completely into absorption, either. The closest it ever came to this was in the one spectrum at MHJD = 8548.856, immediately after the blue wing disappeared and before the absorption wings became recognizable, about 100 min after

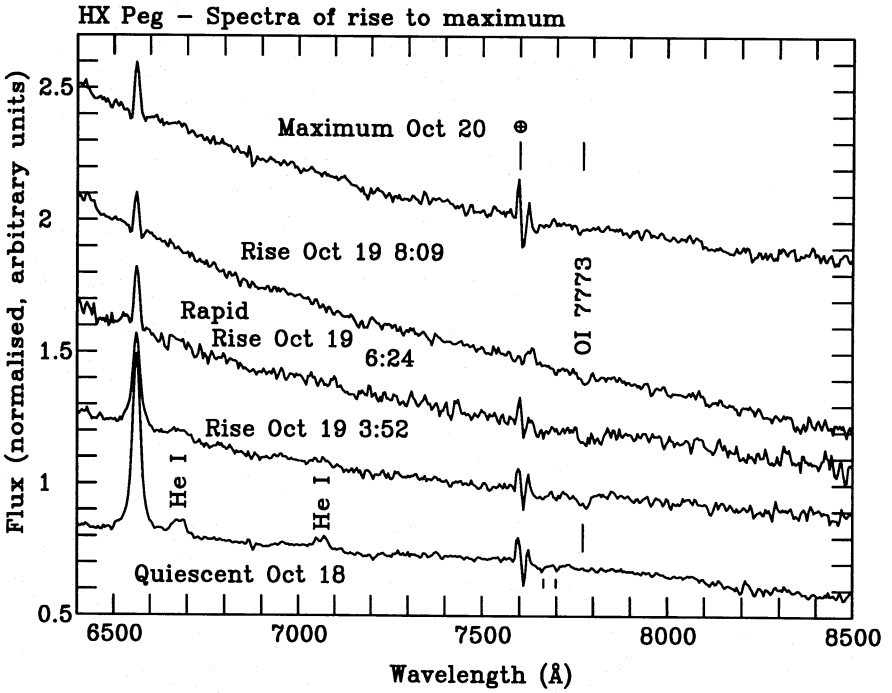

Figure 5. Spectra of HX Peg, all normalized to λ7500 Å. The bottom trace is offset downward by 0.25 flux units, and the third, fourth, and fifth from bottom are offset upwards by 0.25, 0.5 and 1.0 units, respectively, for clarity. Wrinkles from imperfect removal of the telluric A-band near λ7600 Å are marked by ⊕. The bottom trace comprises all spectra from 1991 October 18 UT. Progressing upward are the next nights' spectra, with UTs of mid-exposure shown. The trace at 3:52 UT, marked 'Rise', comprises the spectra taken from the beginning of the night (MHJD 8548.581) to MHJD 8548.729, spanning 3.6 h. The trace at 6:24 UT, marked 'Rapid Rise', comprises the spectra taken from MHJD 8548.741 to 8548.787, spanning 1.1 h. This trace represents a sudden brightening in the spectrum in this brief time. Note O I λ7773 Å in broad absorption, during the previous gradual brightening. The trace at 8:09 UT, marked 'Rise', comprises the spectra taken from after the rapid rise (MHJD 8548.798) to the end of the night (HJD 8548.890), spanning 2.2 h. The top trace comprises all spectra taken on the final night.

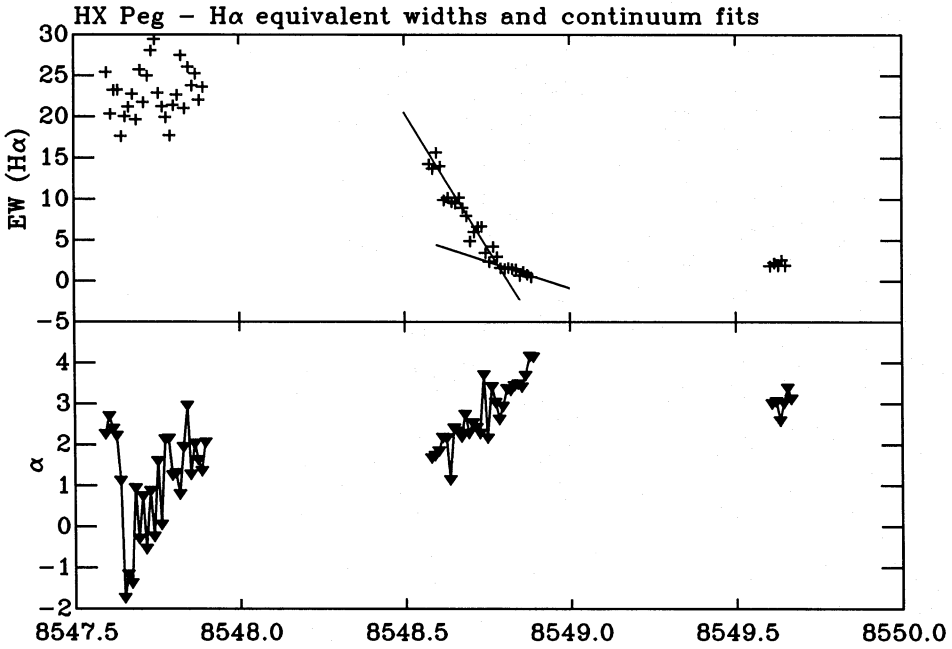

Figure 6. Top: equivalent widths of Hα plotted against MHJD. The observations on 1991 October 18, 19 and 20 UT readily indicate minimum, rise into high state, and maximum. The fitted lines change slope at the onset of the rapid rise. Bottom: continuum slope, measured by index α by fitting a power law $F_\lambda = k\lambda^{-\alpha}$ to the continuum over $\lambda\lambda$6350–6450 and 6750–6850 Å, plotted against MHJD.

the rapid rise. The line centre went into absorption extending below the continuum level, at -650 km s^{-1} relative to the rest frame, but still with emission wings at -400 and $+530$ km s^{-1} to either side of it.

The behaviour of the continuum slope in F_λ (Fig. 6) contrasts with that seen by MK90. The continuum slope of TW Vir was nearly constant until the rapid rise, and then kinked to the blue; the continuum slope for HX Peg rose more steadily. It was measured by index α of a power law, $F_\lambda = k\lambda^{-\alpha}$, with errors of ± 0.5, of a fit to the continuum over $\lambda\lambda$6350–6450 and 6750–6850 Å (see Table 1). These spectral regions were chosen to avoid Hα, telluric absorption, and strong night-sky emission lines, which might have left ripples after sky subtraction.

Curiously, during the night before the rise to maximum, the continuum slope reddened suddenly and then became blue. If this was solely due to an atmospheric refraction effect through the unrotated slit, one might expect to see it the next night, too. It was not, even though the hour angles (H) swept through were similar, from $H = -3{:}24$ to $+3{:}53$ h on the first night, and from $H = -3{:}38$ to $+3{:}48$ h on the second night. There is also no obvious correlation between equivalent widths and continuum slopes on the first night.

7 DISCUSSION

These observations resemble those of MK90 in that this CV was caught during a rapid rise to a high state. Both TW Vir and HX Peg showed a gradual brightening of the continuum before this, as had also been seen by Clarke, Capel & Bowyer (1984) and Kaitchuck, Mansperger & Hantzios (1988). Such a pattern is consistent with the theory of warm and hot phases in the dwarf nova outburst (Mineshige 1988). This theory was intended to explain the UV delay of dwarf nova outbursts (Hassall et al. 1983), in the context of the disc instability model.

There are differences, however. The observed kink in the Hα equivalent width curve contrasts with the smooth transition of the line fluxes of MK90. The continuum slope of MK90 showed an abrupt transition at the rapid rise, whereas that of HX Peg shows a wiggle on a steady increase in an already blue continuum.

Two important time-scales to constrain are the time between the onset of the warm phase and the onset of the hot phase, and the time between the onset of the hot phase and maximum light. If the time of the kink in the equivalent width curve is the onset of the hot phase, and also if the drop and rise in the equivalent width curve seen shortly after the beginning of the first night mark the onset of the warm phase, this suggests an interval for the first time-scale of 27.3 h. The models of Mineshige (1988) and the observations of MK90 suggest a time-scale of about 24 h, tantalizingly close to this. The onset of the warm phase has never been seen before, though, and caution must be used with any 24-h time-scale: since one cannot observe in the daytime, this time-scale will be imposed on the data by the convolution theorem (see Press et al. 1992). If the onset of the warm phase was missed in the intervening daytime, a lower limit of at least 4.9 h can be set, by the beginning of observations on the second night. The interval between the onset of the hot phase and maximum light is similarly constrained, to between 2.5 and 19.7 h. While this longer time-scale is also consistent with the models of Mineshige and the observations of Mansperger & Kaitchuck, detailed modelling is outside the scope of this work. The fits of MK90 involve five adjustable parameters,

plus system parameters such as stellar masses and radii, and orbital inclination, which are difficult to determine in even the most careful analyses (e.g. Wade & Horne 1988).

The red coverage allowed O I λ7773 Å to be observed, which became detectable in absorption during the rise to maximum. For the successive averages of spectra taken on October 19, shown in Fig. 5, the equivalent widths were -1.6, -2.2 and -1.2 Å, respectively, all with errors of ± 0.5 Å. This quintuplet probably forms in CV accretion discs, since it is sensitive to outburst state (Friend et al. 1988), much as the higher Balmer lines are (e.g. Szkody, Piché & Feinswog 1990). In the Sun, this feature forms at the boundary between the chromosphere and the photosphere, as shown by the solar flash spectrum (Bray & Loughhead 1974). This may explain its sensitivity to surface gravity: it has long been used as a luminosity-class indicator for supergiants (Keenan & Hynek 1950), and can be used over a wide range of spectral types, from B to K (Thomas, Morton & Murdin 1979). Its sensitivity to CV outburst state might be explained by accretion discs becoming optically and geometrically thick during outburst (Smak 1992). There is some evidence that it forms in the outer disc (Marsh 1990), at least in one quiescent dwarf nova. In HX Peg, O I λ7773 Å was in absorption during the warm phase, before the rapid rise to maximum. If this feature really does form in the outer disc, this is consistent with a brightening in the outer disc in the early stages of the rise to maximum. The outburst may therefore have started in the outer disc and moved inward.

ACKNOWLEDGMENTS

This work is based on a chapter in the author's PhD thesis, from the Department of Physics and Astronomy, Dartmouth College. The author was the recipient of a Dartmouth Fellowship when the spectra were taken, and now holds a PPARC Post-Doctoral Research Fellowship. Analysis was carried out on the Keele STARLINK node using the ARK software. The spectra were taken at the Michigan–Dartmouth–MIT Observatory, which is owned and operated by a consortium of the University of Michigan, Dartmouth College, and the Massachusetts Institute of Technology. I thank Bob Barr, Peter Mack and Larry Breuer for observatory support, John Thorstensen and Tim Naylor for software, Cathy Mansperger and Ron Kaitchuck for helpful discussions, and Lola Eachus Chaisson and William Liller for writing to me about their study in the Harvard College Observatory plate archive. Special thanks are due to Mrs Chaisson, for giving permission to publish the plot of the magnitudes she painstakingly measured. I also thank Josh Grindlay for keeping her notebook in a box filled with other treasures in his office for over ten years. That in late 1993 I was able to find this notebook and its measurements made in 1975 – and make use of them – is indeed part of what makes this science of astronomy so interesting.

REFERENCES

Bath G. T., 1973, Nat. Phys. Sci., 246, 84
Beuermann K., Thorstensen J. R., Schwope A. D., Ringwald F. A., Sahin H., 1992, A&A, 256, 442
Bray R. J., Loughhead R. E., 1974, The Solar Chromosphere. Chapman and Hall, London, p. 165
Cash W., 1979, ApJ, 228, 939
Clarke J. T., Capel D., Bowyer S., 1984, ApJ, 287, 845
Friend M. T., Martin J. S., Smith R. C., Jones D. H. P., 1988, MNRAS, 233, 451
Green R. F., Greenstein J. L., Boksenberg A., 1976, PASP, 88, 598 (GGB76)
Green R. F., Schmidt M., Liebert J., 1986, ApJS, 61, 305
Greenstein J. L., Arp H. C., Shectman S., 1977, PASP, 89, 741 (GAS77)
Hassall B. J. M., Pringle J. E., Schwarzenberg-Czerny A., Wade R. A., Whelan J. A. J., Hill P. W., 1983, MNRAS, 203, 865
Honeycutt R. K., Robertson J. W., Turner G. W., Vesper D. N., 1994, in Shafter A. W., ed., ASP Conf. Ser. Vol. 56, Interacting Binary Stars. Astron. Soc. Pac., San Francisco, p. 277
Howell S. B., Szkody P., 1990, ApJ, 356, 623
Kaitchuck R. H., Mansperger C. S., Hantzios P. A., 1988, ApJ, 330, 305
Keenan P. C., Hynek J. A., 1950, ApJ, 111, 1
la Dous C., 1993, in Hack M., la Dous C., eds, Cataclysmic Variables and Related Objects. NASA/CNRS Monograph Series on Non-Thermal Phenomena in Stellar Atmospheres, NASA
Liller W., Eachus L., 1976, IAU Circ. 2907
Luppino G. A., 1989, PASP, 101, 931
Mansperger C. S., Kaitchuck R. H., 1990, ApJ, 358, 268 (MK90)
Marsh T. R., 1990, ApJ, 357, 621
Mattei J., 1990, in Ibanoglu C., ed., Active Close Binaries. Kluwer, Dordrecht, p. 611
Mineshige S., 1988, A&A, 190, 72
Oke J. B., 1974, ApJS, 27, 21
Oke J. B., Gunn J. E., 1983, ApJ, 266, 713
Osaki Y., 1974, PASJ, 26, 429
Patterson J., 1984, ApJS, 54, 443
Press W. H., Teukolsky S. A., Vetterling W. T., Flannery B., 1992, Numerical Recipes in FORTRAN, Second Edition. Cambridge Univ. Press, Cambridge, p. 569
Ringwald F. A., 1993, PASP, 105, 805
Ritter H., 1990, A&AS, 85, 1179
Schneider D. P., Young P. J., 1980, ApJ, 238, 946
Shafter A. W., 1983, ApJ, 267, 222
Shafter A. W., Wheeler J. C., Cannizzo J. K., 1986, ApJ, 305, 261
Smak J., 1984, PASP, 96, 5
Smak J., 1992, in Kondo Y. et al., eds, Evolutionary Processes in Interacting Binary Stars. Kluwer, Dordrecht, p. 83
Szkody P., Piché F., Feinswog L., 1990, ApJS, 73, 441
Thomas R. M., Morton D. C., Murdin P. G., 1979, MNRAS, 188, 19
Thorstensen J. R., Freed I. W., 1985, AJ, 90, 2082
Thorstensen J. R., Davis M. K., Ringwald F. A., 1991a, AJ, 102, 683
Thorstensen J. R., Ringwald F. A., Wade R. A., Schmidt G. D., Norsworthy J. E., 1991b, AJ, 102, 272
Wade R. A., Horne K., 1988, ApJ, 324, 411
Warner B., 1987, MNRAS, 227, 23